Flomeko 2000 - IMEKO TC9 Conference
Salvador, Bahia, BRAZIL
4-8 June, 2000

THE ULTRASONIC CROSS-CORRELATION FLOW METER – NEW INSIGHTS INTO THE PHYSICAL BACKGROUND

V. Skwarek, V. Hans
University of Essen
Institute for Measurement and Control
45117 Essen, Germany

Abstract: During the last years of research, flow measurement by the cross correlation method made much progress concerning accuracy and reliability. Especially for gaseous fluid the signal processing was far improved by new demodulation techniques such as undersampling and complex demodulation. This allows new insights into the physical principle of interaction between ultrasound and fluid introduced in this paper.

Keywords: ultrasound cross-correlation flow measurement, complex demodulation, Hilbert-transform, interaction ultrasound-fluid

1 INTRODUCTION

Cross-correlation measurement techniques are very common and often used in all branches of measurement science. Generally, they compare two given patterns for similarities between referring points. For different time shifts t between the signals a result function

$$f_{s1s2}(t) = \lim_{T\to\infty} \frac{1}{2T} \int_{-T}^{T} s_1(t) s_2(t-t)\,dt \tag{1}$$

called cross-correlation-function (CCF) is obtained. The maximum of the CCF indicates the maximum similarity in arbitrary units of the input signals. Usually they are standardized to a maximum range between –1 and 1 by

$$f_{s1s2,stand}(t) = \frac{f_{s1s2}(t)}{\sqrt{f_{s1s1}(0) f_{s2s2}(0)}}\,. \tag{2}$$

The cross-correlative measurement method does the same using ultrasound: Two continuous ultrasonic beams are sent radially through the pipe with the streaming fluid (figure 1). As they are installed within a short distance to each other, both beams are expected to be modulated similarly by any disturbances in the fluid.

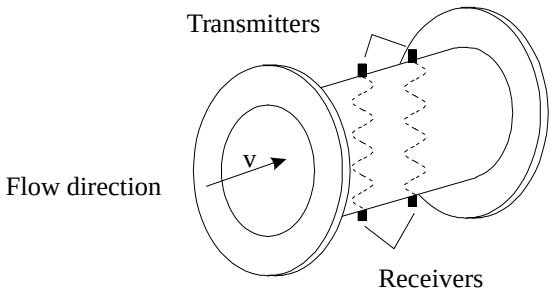

Figure 1: Measurement Setup.

During the first steps of research for this kind of correlation measurement [1] macroscopic influences such as particles or bubbles were required. Changes of ultrasound had to be of a high magnitude for evaluation with a sufficient result. Due to improvements of signal processing it is meanwhile possible to detect also turbulent structures in gaseous fluids. Their low modulation depth of less than 10% compared with particle flows requires a separation of the load signal from the carrier. Otherwise, the high self-similarity of the unchanged carrier produces a higher peak in correlative evaluation (figure 2 left) than the similarity caused by stochastic turbulences (figure 2 right).

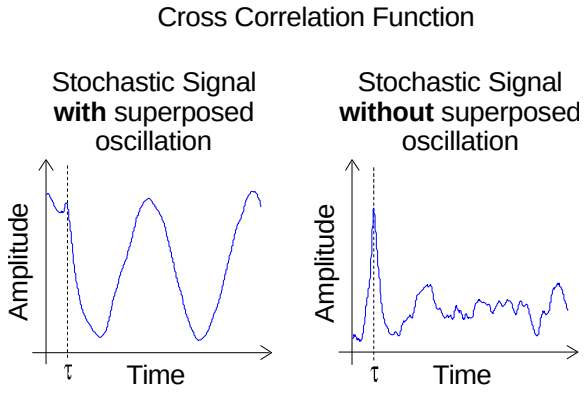

Figure 2: Cross correlation of stochastic signals with (left) and without (right) superposed oscillation such as a carrier or pulsation.

With such an improved signal processing [2] results of a much higher quality than before are obtained. These results again can be used for building better models about the physical principle of the ultrasonic flowmeter

The main topic of this paper is an explanation of the new and improved facilities. Therefore, the next section gives a short description about basic innovations concerning the evaluation and processing of the signals. Then an extended model is presented which helps to understand the cross-correlation flow metering principle on the basis of ultrasound-turbulence interaction. Finally, a conclusion will give some intention about aims of future research.

2 IMPROVED SIGNAL PROCESSING

As already said before the main improvement for cross-correlative determination of average gas flow bases on the demodulation of the required signal portions. Originally [1], this fact was neglected so that the modulated carrier was processed entirely. The consequences as shown in figure 2 are proven in the following calculations:

Usually a modulation is expressed by

$$s(t) = a(t)\sin(wt + j_0 + j(t)) \tag{3}$$

with the amplitude modulation (AM) *a(t)* and the phase modulation (PM) $j(t)$. Alternatively it can be written as a sum of sinusoidal signals with a different frequency and phase shift

$$s(t) = \sum_i a_i(t)\sin(w_i t + j_i(t)) \tag{4}$$

by the means of a *Fourier* decomposition.

Now, a virtual signal

$$s(t) = x(t) + y(t) \tag{5}$$

is considered consisting of a carrier *x(t)* and the modulation *y(t)* with the magnitude and the frequency of the carrier by a factor 10 higher than the entire rest of the signal. For reasons of simplitcity the “rest” is reduced to a virtual stochastic function.

The signals

$$s_2(t) = s_1(t+\tau) = x(t+t_i) + y(t+t_j) \tag{6}$$

are the same at both barriers apart from an individual time shift τ. The time shift t_i equals to zero because the transmitters at all barriers are excited by the same electric signal without any measurable delay.

These considerations reduce the cross-correlation to an auto-correlation (ACF)

$$f_{s1s1}(\tau) = \lim_{T\to\infty}\frac{1}{2T}\int_{-T}^{T} s_1(t+\tau)s_1(t)dt\,. \tag{7}$$

The effects on equation (5) are obvious. It results into a permutation of correlations between all subfunctions:

$$f_{s1s1}(\tau) = \lim_{T\to\infty}\frac{1}{2T}\int_{-T}^{T}\big(x(t)+y(t)\big)\big(x(t)+y(t+t_j)\big)dt,$$

$$f_{s1s1}(\tau) = \lim_{T\to\infty}\frac{1}{2T}\int_{-T}^{T} x(t)x(t)+x(t)y(t+t_j)+y(t)x(t)+y(t)y(t+t_j)dt. \tag{8a/b}$$

Understanding the products in the integral as single correlations, equation (8b) changes into

$$f_{s1s1}(t) = f_{xx}(t_i) + f_{xy}(t_j) + f_{yx}(t_i) + f_{yy}(t_j). \quad (9)$$

Due to the independency of *x(t)* and *y(t)* their CCF equals to zero and equation (9) is simplified to

$$f_{s1s1}(t) = f_{xx}(t_i) + f_{yy}(t_j). \quad (10)$$

This proves the results as displayed in figure 2 showing the superposition of CCFs between a sine and a stochastical functions. Obviously the carrier with the higher amplitude determines the position of the maximum. Therefore, carrier based signals with small modulation depths require a separation of carrier and load signal otherwise their influence will not be taken into account at a correlative evaluation.

A very basic technique for demodulation called “carrier-synchronized undersampling with integer submultiples of the carrier frequency” was used by *Poppen* [3] and *Rettich* [4] with good success during their research. Generally, it uses the phenomenon of a repeating frequency spectrum in a sampled signal. The gap between the repeating bands is equivalent to the sampling frequency. A subdivision of this frequency by an integer number shifts one of these bands to *f = 0* Hz. Then the redundant pictures can be suppressed by high pass filtering and the load signal is demodulated to its original band (figure 3).

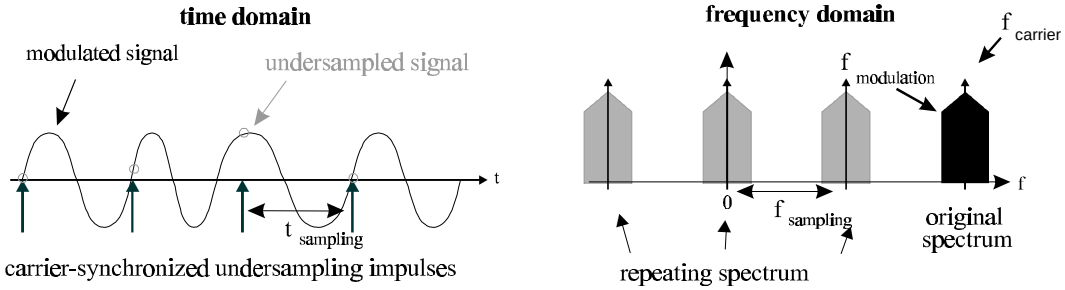

Figure 3: Undersampling in time- and frequency domain.

However, according to equation (3) this method does not pay any reapect to the fact that a signal may be modulated in amplitude and phase but the “modulation” is only treated as one part. With the independence of AM and PM part of a signal as proven in [2], [5] and [6], their common evaluation will lead to non-negligible deviations. This can easily be understood by assuming the ultrasonic signal as an exchange of impacts on an atomic basis, also called phonons. Such phonons are bound to mass underlying influences such as friction or movement. Therefore properties of ultrasound are defined and modified as following:

- The amplitude indicates the “energy contents”. The power density is reduced as well by absorption due to atomic friction as by the expansion of the wavefront.
- The phase depends on propagation properties defined by speed of sound.

Generally, both effects can appear independently so that better results are to be expected for a separate demodulation.

One of the main results in [2] is the examination of an extended demodulation technique which is able to separate the signals by amplitude and phase. This technique is called “complex demodulation” and interprets a carrier in the complex domain. There, the signal is represented by a phasor with a changing amplitude and phase (figure 4).

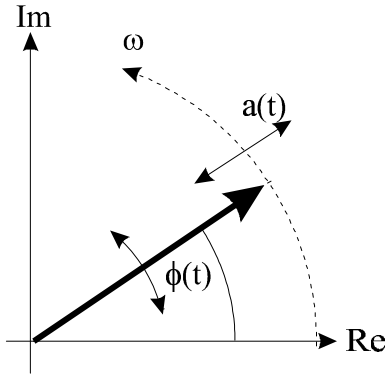

Figure 4: Amplitude and phase modulated signal in complex domain.

Undersampling with integer submultiples of the carrier frequency fixes the phasor – a rotating pointer – at a defined phase because only one sample per one or more rotations is taken. Now, the AM- and PM-portion are obtainable directly from the complex domain via real- and imaginary part of the sample as the temporal change of amplitude and phase:

$$j(t) = \arctan\frac{\mathrm{Im}\{\underline{s}(t)\}}{\mathrm{Re}\{\underline{s}(t)\}}, \qquad a(t) = \sqrt{\mathrm{Re}\{\underline{s}(t)\}^2 + \mathrm{Im}\{\underline{s}(t)\}^2}. \tag{10 a/b}$$

But the measurement of the imaginary part in real applications becomes problematic because they cannot be directly obtained. Therefore an electronic *Hilbert*-transform has to be used to reconstruct both components. Without giving a detailled proof [2], [7], [8], this method gives a correlation between real- and imaginary-parts for measures in a causal system: the convolution

$$Hilbert\{\underline{s}(t)\} = \underline{s}(t) * \frac{1}{p\ \arg(\underline{s}(t))} \tag{11}$$

returns after a series of calculations an auxiliary function *M(t)* defining

$$\mathrm{Re}\{M(f)\} = Hilbert\{\mathrm{Im}\{M(f)\}\}, \qquad \mathrm{Im}\{M(f)\} = -Hilbert\{\mathrm{Re}\{M(f)\}\}. \tag{12 a/b}$$

An electronic realization of a *Hilbert*-transform for carrier based signals is suggested by *Otnes* [7]. He does not transform the modulated signal directly but multiplies it with the *Hilbert* transform of the carrier (figure 5). A final low pass filter separates the desired load signals.

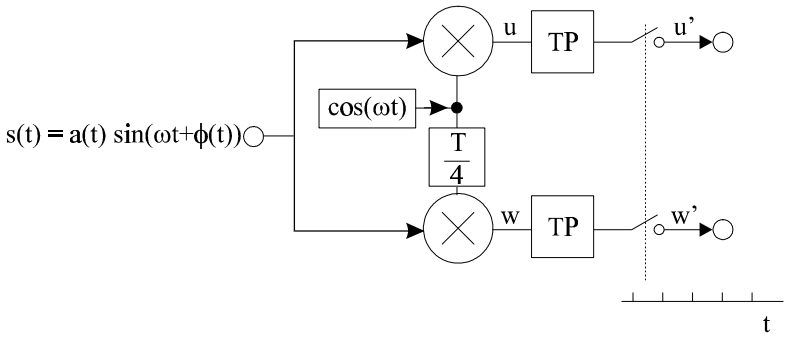

Figure 5: Block diagram for electronic *Hilbert*-transform.

The application of trigonometric theorems clarifies this argumentation. A signal according to equation (3) is split in two subchannels

$$u(t) = a(t)\sin(wt + j(t))\sin(wt), \qquad w(t) = a(t)\sin(wt + j(t))\cos(wt) \tag{13 a/b}$$

which are multiplied again with the carrier and its *Hilbert*-transform, respectively. These equations are transformed to

$$2u(t) = a(t)(\cos(j(t)) - \cos(2wt + j(t))), \qquad 2w(t) = a(t)(\sin(j(t)) + \sin(2wt + j(t))). \tag{14 a/b}$$

A high-pass filter eliminates the terms of double the carrier frequency and a so-called *Hilbert*-couple remains. Expectedly, the *Hilbert*-couple completes the complex oscillation

$$\frac{a(t)}{2}e^{(j(t))}. \tag{15}$$

According to the results above, these signals are equivalent to real- and imaginary-part of the original signal. Consequently, the desired AM and PM portions are calculated by simultaneous sampling of both channels and further processing of the obtained data according to equations (10 a/b).

Results for measurements with the new demodulation algorithms are displayed in figure 6. As the sampling-in-zero-crossings method also called single-point-sampling was used for the demodulation of the PM part of the signal, the comparison refers also to the PM part of the complex demodulation. In the top left diagram the calibration curve is shown as an average over 100 measurements for different fluid velocities. It indicates the ratio between measured and reference values and a calibration free principle ideally equals to one. Though the new method still obviously

differs from an ideal measurement the course of the graph is much more regular than in the original principle.

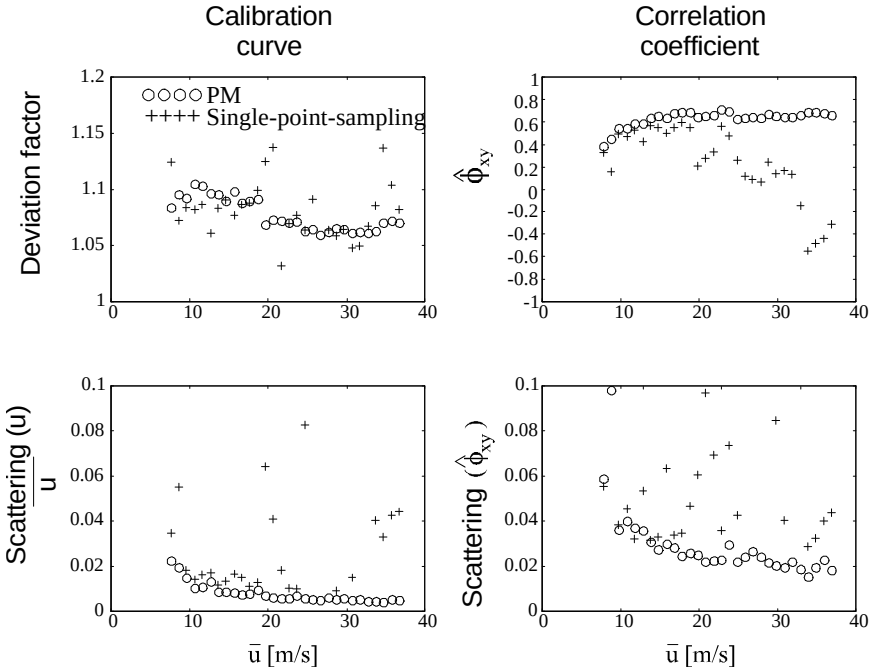

Figure 6: Comparison of results obtained by single-point-sampling or direct phase demodulation.

Much more important than the calibration curve is the scattering in the lower left diagram. Unlike systematic deviations the scattering is not compensatable by look-up tables or other calibration precautions. It has to be kept as low as possible otherwise the industrial use especially for billing applications is restricted. A device cannot be gauged if the scattering exceeds very tight limits of usually below 5% of the current measure. With the new demodulation principle scattering could be far reduced compared with the former principle. Not only that the absolute values are smaller but the course of the graph is far more asymptotic for higher velocities which is an decisive property for gauging.

The reason for the different behavior of the old and the new device is given in the upper left diagram by the correlation cofficient in the maximum of the CCF: The old principle first increases up to a velocity of about 15m/s with a growing scattering. Then it drops suddenly down to zero and takes on negative values.

Sensor movement explains this behavior of the correlation coefficient. As already mentioned before, the old principle is sensitive on the absolute sampling phase. With minimally moving sensors at a wavelength of 1.5 mm vibrations on the pipe, temperature caused extension or sucking due to underpressure of the fluid cause absolute phase shifts of more than 90°. Exceeding these values the single-point-sampling becomes ambiguous because it projects the amplitude of a sine function on its phase. Therefore, an increasing phase shows the same effect as a decreasing phase. This is disadvantageous for similarity considerations because no physical similarity is guaranteed for apparent mathematical similarities. Consequently no similar sections are detected in the signals making the CCF drop down to zero. Further movements cause one transmitter sampled at the rising edge while the other is sampled at the falling edge of a sine. Now similarities are inversed with a negative result of the correlation.

The new method in contrast calculates unique angles over an infinite range by calculating the ratio of two consequent samples. Although the used tangent function in equation (10 a) is also ambiguous (figure 7) singularities indicate an exceeded unique range. Therefore, reconstruction algorithms are used to detect such singularity steps and extend the angular domain to infinity.

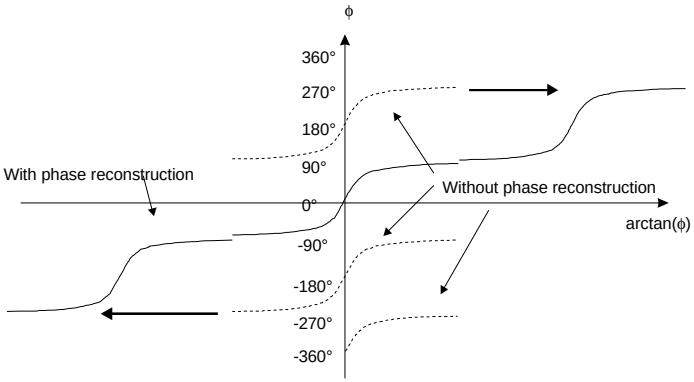

Figure 7: Principle of phase reconstruction for arctan-function.

3 MODELS ABOUT THE WORKING PRINCIPLE

There are still many myths about the cross-correlation flow meter and the exact working principle. Although a vast number of models was formed no explanation of physical backgrounds could be given because the interaction of ultrasound and fluid is very complex. The question about "what is really measured" is still unanswered. With the separation of the signal into amplitude and phase influenced parts, a new model has to be offered explaining their origin.

Due to the extended possibilities of signal processing it is now possible to separate a modulated signal into its amplitude and phase modulating portions. In accordance to *Poppen* the original intention of the flowmeter was kept which was the determination of the average flow speed by analyzing the phase shifts of signals. Therefore, only the phase of the complex demodulation was evaluated.

In this section similarities between AM- and PM-causing "structures" are examined for finding the best way for further signal analysis. The phrase "structures" is used intentionally although one has to be aware that no discretely definable structures such as in a *Karman*-vortex street exist. A fluid is rather a mixture of inhomogenities of different scales which are not clearly separable by different structure models. Consequently, models using "structures" are always a simplification of reality according to human imagination.

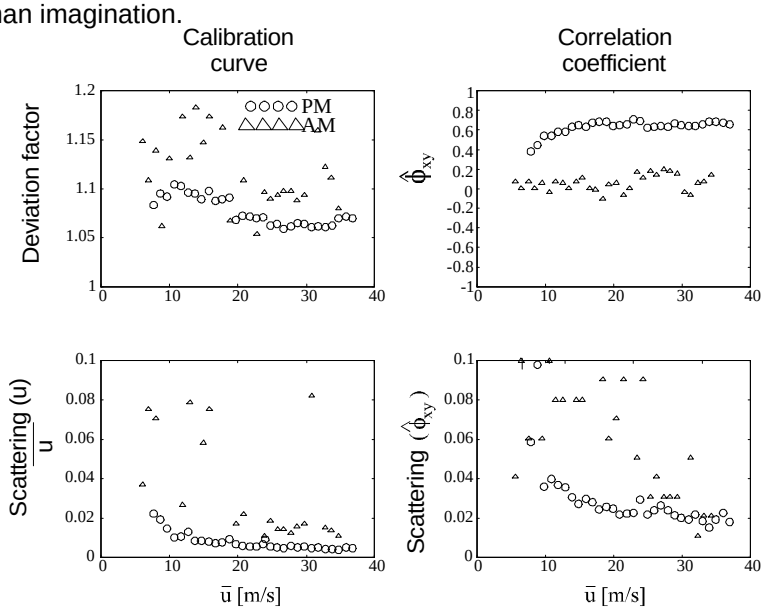

Figure 8: Comparison of AM- and PM-portion of a modulated signal.

In figure 8 a diagram similar to figure 6 is shown, now comparing the demodulated amplitude and phase. Without getting lost in details, two significant differences between the curves are obvious:

- Average and scattering of the calibration curve in the left hand diagrams indicate a very irregular behavior for the amplitude, scattering much more than the signal phase.
- Similar to considerations about the difference between the old and new principle, high scattering is caused again by a very low correlation coefficient in the maximum of the CCF.

According to these observations there are two possible explanations for such a behavior: Either AM is much more sensitive than PM so more physical influences are included in this signal part. But with a higher number of influences it has to be expected that the correlation between two barriers in a certain distance decreases because it is improbable that all influences stay similar. Or AM and PM have no common features and AM registers influences with a far reduced stability than PM.
The first case can be checked by a modified cross correlation technique. Not the first and second barrier are now compared for similarities but AM and PM at the same barrier. With equal influences a significant maximum nearby $t = 0$ has to be expected. In figure 9 results of such examinations can be seen. Although there is a maximum at $t = 0$ it is neither very significant nor was it caused by influences of the fluid. There were rather simultaneous disturbances at all channels caused by the signal processing hardware. Consequently, the same influences for AM and PM are excluded.

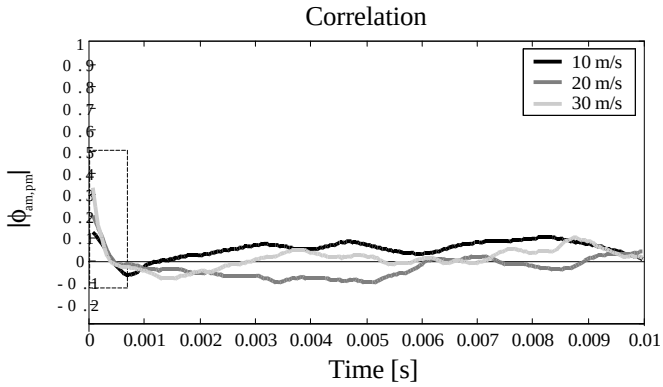

Figure 9: Correlative comparison of AM and PM part of one signal at the same barrier.

The explanation is assumed as the second case concerning dissipating structures for AM. *Fiedler* [9] suggests to use micro- and macroscales for a rough estimation of structures sizes. The macroscale is defined as the area of a spatial correlation function and gives information about most influencing structures. Microscales are graphically approximated by the section between a parabolic approximation to the correlation function and the abscissa. Results can be seen in the following table:

	Microscale	**Macroscale**
AM	6 mm	6 mm
PM	10 mm	25 mm

There the reason for the different behavior is obvious: AM is sensitive to very small structures with a scale nearby the wavelength of the used ultrasound. Furthermore the main information is carrier by dissipating structures. Consequently, no similarities can be found between the first and second barrier because most structures are already dissipated before reaching the second ultrasonic beam. Unlike the phase with its main information in large size structures. They stay similar during their propagation through the pipe and can therefore be redetected and cross-correlatively found.
As a final conclusion the phase information seems to be more reliable for a redetection of turbulent structures. Conversely, AM bases on structures dissipating between both barriers so their evaluation is not suitable for this flow measurement principle. Furthermore, it explains the deviations achieved with the former demodulation technique used by *Poppen*. As already mentioned, the accuracy of his method depends on the absolute phase of the sampling point which should be at about 0°. There the PM-part of a signal is demodulated. With a phase shift in direction of 90° an increasing influence of AM is recognized with only amplitude demodulation at an absolute sampling angle of 90°. Consequently, a wrong adjustment of the sensors leads to missing similarities and faulty measures including increased scattering. The new method however demodulates always the PM part without any dependency to the absolute sampling phase.

4 SUMMARY AND OUTLOOK

The cross correlation measurement principle takes a great advantage from a signal separation into amplitude and phase. Compared with former principles not only an independence from the absolute sampling phase is achieved. Much more important is now the possibility of a selective phase evaluation without ambiguity of the calculated angle as usual with the use of trigonometric functions. In combination with the extended model set up for this demodulation technique more reliable results concerning average and scattering are to be expected.

These new possibilities and the presented physical background can be used for further research. It is now possible to apply multiple sensors at the pipe for performing simultaneous multi path measurements. One future aim is a tomographic online visualization of turbulent flow and the modulating influences.

5 ACKNOWLEDGEMENT

The research was supported by the grant of the ”Deutsche Forschungsgemeinschaft” (Forschergruppe ”Strömungsmechanische Grundlagen der Durchflußmessung”, Me 484/29-1).

REFERENCES

[1] M.S. Beck, *Cross Correlation flowmeters: their design and application,* IOP Publishing, Bristol, 1987.
[2] V. Skwarek, *Verarbeitung modulierter Ultraschallsignale in Ein- und Mehrpfadanordnungen bei der korrelativen Durchflußmessung*, PhD thesis, University of Essen, 2000.
[3] G. Poppen, *Durchflußmessung auf der Basis kreuzkorrelierter Ultraschallsignale*, PhD thesis, University of Essen, Shaker, Aachen, 1997.
[4] T. Rettich, *Korrelative Ultraschall-Durchflußmessung auf der Basis turbulenter Strukturen*, PhD thesis, University of Essen, VDI, Düsseldorf, 1999.
[5] V. Skwarek, V. Hans, Modern Principles of Signal Processing for Analyzing Properties of Turbulent Fluids, IEEE-Workshop on Intelligent Signal Processing, pp. 5-10, Budapest/Hungary, 4.-7. September 1999.
[6] Skwarek, V.; Hans, V.: Verarbeitung kreuzkorrelierter Ultraschallsignale bei der Durchflußmessung, Sensoren und Meßsysteme 2000, pp. 639-648, Ludwigsburg/Germany, 13.-14. März 2000.
[7] R. K. Otnes, L. Enochson, *Applied time series analysis,* Wiley, New York/USA, 1978.
[8] W. Bachmann, *Signalanalyse*, Vieweg, Braunschweig, 1992.
[9] H.E. Fiedler, Turbulente Strömungen, 1995.

AUTHORS: Dipl.-Ing. Volker Skwarek, Prof. Dr.-Ing. Volker Hans, University of Essen, Institute of Measurement and Control, Schuetzenbahn 70, 45117 Essen, Germany, phone: ++49-201-183-2897, fax:++49-201-183-2944, E-Mail: volker.skwarek@uni-essen.de, volker.hans@uni-essen.de